GLOBAL JOURNAL OF BIO-SCIENCE AND BIOTECHNOLOGY

www.scienceandnature.org

SYNTHESIS CHARACTERIZATION AND ANTIBACTERIAL ACTIVITY OF IRON OXIDE NANOPARTICLES

Marimuthu Margabandhu[1], Sechassalom Sendhilnathan[2], S. Maragathavalli[3], V. Karthikeyan[4] & B. Annadurai[5]

[1]University College of Engineering, Ariyalur, Kathankudikadu, Thelur, Ariyalur
[2]Anna University, Chennai., Tamil Nadu, Pin code-614701, India. Email: senthilnathan10@yahoo.com.
[3, 4 &5] Research and Development Centre, Bharathiar University,Coimbatore

ABSTRACT
The iron oxide nanoparticles (IONPs) have been synthesized in aqueous solution by co-precipitation method using $CoCl_2$, $MnCl_2$ and $FeCl_3$ mixtures respectively in NaOH solution. The synthesis of iron-oxide nanoparticles were validated by FTIR the frequency bands range between 591-571 cm^{-1} and 435-412 cm^{-1} are attributed to the tetrahedral and octahedral structural vibrations which confirms the presence of metal oxide stretching band in ferrites as valid standard reference. Average sizes of IONPs were determined by using Debye Scherrer's Formula which is in between 14-68 nm particle size. The X-ray power diffraction (XRD) analysis revealed the crystallographic structure of magnetic particles. The average crystallite size decreases with increase in manganese substitution. The Coercivity and Magnetic Retentivity of the particles were measured at room temperature by using VSM. The Coercivity and Magnetic Retentivity (Mr) were found to decrease with the increase in Manganese substitution. Characterization of the mean particle size and morphology of IONPs are confirmed in SEM which shows cubic spinel in shape. Further the antibacterial effect of iron oxide nanoparticles was evaluated against *Escherichia coli* and *Bacillus subtilis* which showed that the nanoparticles have moderate antibacterial activity against both bacterial strains and retains potential application in pharmaceutical and biomedical industries.

KEYWORDS: Iron oxide nanoparticle (IONPs), coprecipitaion, *Escherichia coli, Bacillus subtilus.*

INTRODUCTION
Nanotechnology is the science that deals with manipulating matter at the atomic and molecular scale and the size range between 1- 9nm. Magnetic nanoparticles of iron oxides (Fe_3O_4 and Fe_2O_3) are now extensively used throughout the medicine, drug delivery systems, superparamagnetism, antimicrobial, non-toxicity, biocompatibility, biodegradability properties and low price. (Kluchova *et al*., 2009; Zhang and Zhang, 2005) Bacterial infections were one of the major causes of mortality in the nineteenth century. Antibiotics, which were discovered in the middle of the nineteenth century, successfully reduced the mortality caused by bacterial diseases. Nowadays, antimicrobial effects are intensively studied due to an enormously increasing bacterial resistance against excessively and repeatedly used classical antibiotics. It is very complex and the evolutionary processes usually occur during antibiotic therapy, leading to the emergence of heritable resistance to antibiotics. Horizontal gene transfer (HGT) through bacterial conjugation, transduction, transformation or biofilm formation can spread drug resistance (Seil and Webster, 2012). In the presence of chemical agents the interfacial and surface properties can be modified. Indirectly, such agents can stabilize against coagulation and aggregation by maintaining particle charge and by modifying the outermost layer of the particle (Sophie Laurent *et al*., 2008). Iron oxide nanoparticles have been of great interest, not only for fundamental properties caused by their multivalent oxidation states but also for their super paramagnetic, high force, low Curie temperature, high magnetic susceptibility, etc. (Gupta and Gupta, 2005). Iron oxide nanoparticles are of particular interest as antibacterial agents, as they can be prepared with extremely high surface areas and unusual crystalline morphologies with a high number of edges and corners, and other potentially reactive sites (Velmurugan *et al*., 2010). They have a positive surface charge to facilitate their binding to the negatively charged surface of the bacteria which may result in an enhancement of the bactericidal effect (Stoimenov *et al*., 2002; Seil, and Webster, 2012).

MATERIALS & METHODS
Chemicals
For the synthesis of *IONPs*, Cobalt (II) chloride ($CoCl_2$), Manganese (II) chloride ($MnCl_2$) and Iron (III) chloride ($FeCl_3$) were purchased from sigma Aldrich Pvt Ltd. NaOH, nutrient broth were purchased from HIMEDIA, India**.**
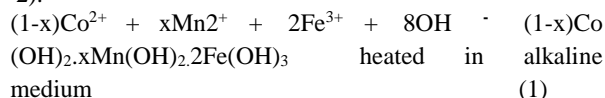### Glassware and Apparatus
All glass wares such as measuring cylinders, test tubes, conical flasks, and beakers etc. were purchased from Borosil, India.
Bacterial Strains
The test organisms *Bacillus subtilis* (MTCC 736) and *Escherichia coli* (MTCC 443) were purchased from Institute of Microbial Technology (IMTECH), Chandigarh, India, and maintained constantly on nutrient agar slant for further use.

Synthesis of Iron oxide nanoparticles

The magnetic nanoparticles synthesized by co-precipitation method specifically based on parameters such as reaction temperature, pH of the suspension, initial molar concentration *etc*. (Vaidyanathan *et al*., 2007). Magnetic nanoparticles of $Co_{1-x}Mn_xFe_2O_4$ with different concentration from 0.0, 0.2, 0.4, 0.6, 0.8, and 1.0 were prepared by co-precipitating aqueous solutions of $CoCl_2$, $MnCl_2$ and $FeCl_3$ mixtures respectively in NaOH solution. The mixed solution consists of $CoCl_2$, $MnCl_2$ and $FeCl_3$ in their respective stoichiometry (For *e.g*., 100 mL of 0.6 M $CoCl_2$, 100 mL of 0.4 M $MnCl_2$ and 100 mL of 2M $FeCl_3$ in the case of $Co_{0.6}Mn_{0.4}Fe_2O_4$ and similarly for the other values of x) was prepared. This mixture was added to the boiling solution of NaOH maintained at 60ºC (0.5 M dissolved in 1000 mL of distilled water) with in the period of 20 seconds under constant stirring. Nano ferrites are formed by conversion of metal salts into hydroxides, which takes place immediately, followed by transformation of hydroxides into ferrites. At first solid hydroxides of metals in the form of fine particles were obtained by the coprecipitation of metal cations in alkaline medium (coprecipitation step) (Equations 1 and 2).

$(1-x)Co^{2+} + xMn2^+ + 2Fe^{3+} + 8OH^- \rightarrow (1-x)Co(OH)_{2.}xMn(OH)_{2.}2Fe(OH)_3$ heated in alkaline medium (1)

$Co_{(1-x).}Mn_{x.}Fe_2O_{4.}.nH_2O$ (2)

The solution was maintained at 85°C for one hour. This duration was sufficient for the transformation of hydroxides into spinel ferrite (dehydration and atomic rearrangement involved in the conversion of intermediate hydroxide phase into ferrite). Sufficient amount of fine particles were collected at this stage as precipitate and added with dilute Hcl to maintain the pH 7.0 the particles were segregated using magnetic separation. These particles were washed with distilled water followed by acetone and dried at room temperature.

Characterization of Iron oxide nanoparticle

X-ray Diffraction

The X-ray diffraction (XRD) patterns of the samples were recorded on a X' PERT PRO X-ray powder diffract meter using Cu K∝ (= 1.54060 Å) radiation. Scanning was made for the selected diffraction peaks which were carried out in step mode (step size 0.05°, measurement time 10 seconds, measurement temperature 25 °C). The crystallite size of the nanocrystalline samples was measured from the X-ray line broadening analyses using Debye- Scherrer formula after accounting for instrumental broadening (Equation 3):

$$D_{XRD} = \frac{0.89}{\cos} \quad (3)$$

Where - wavelength of X-ray used in Å, – is the line broadening at half the maximum intensity (FWHM in radians in the 2 scale), - the Bragg angle, D_{XRD} - crystallite size in nm. The lattice constant (a_o) was determined for various values of Mn content. Co-Mn

ferrite has a spinel structure (Vaidyanathan *et al*., 2007; Morais *et al*., 2001).

Vibrating Sample Magnetometer

Magnetic measurements were carried out at room temperature with a maximum magnetic field of 20000 (G) carried out using a Lakeshore vibrating sample magnetometer (VSM) (model 7404) and parameters like specific saturation magnetization (M_s), coercivity (H_c) and remanence (M_r) were evaluated.

FTIR Spectra

FTIR spectra were recorded for the dried samples of $Co_{1-x}Mn_xFe_2O_4$ with x varying from 0.0 to 1.0 with Lambda 35 spectrometer (range 400 - 4000 cm^{-1}) with data interval of 1.0nm and scan speed 960.00nm/min. The dried samples were in KBr matrix, and spectra were measured according to transmittance method.

Scanning Electron Microscopy

The morphological features of chemically synthesized *IONPs* were studied by using FE-SEM (FEI NOVA Nano SEM)

Growth Kinetic Study by Iron oxide Nanoparticles

The growth kinetic study of *B. subtilis* and *E. coli* was done using different concentrations of *IONPs*. Different concentrations of nanoparticles were added at mid log phase of bacteria and kinetic study was performed at regular time interval of 1 hour by using plate reader (Carry 100, Agilent, USA).

Sample Preparation for Phase Contrast Microscopy

Cultures of *B. subtilis* and *E. coli* were started and at the mid log phase *IONPs* were added and kept for overnight growth. One drop of culture was taken and put on the glass slide for phase contrast microscopic study

RESULTS & DISCUSSION

X-ray Diffraction

Crystalline structure of nanoparticles can be determined by using XRD from which the average size of all the nanoparticles can be estimated. The sizes of the precipitated particles were characterized by using XRD for its structural determination. All the obtained experimental peaks were compared with theoretically generated peaks and they were processed using powder X (Dong, 1999) and indexed with origin software. The lattice constant (a_o) was calculated using the 'd' value and with their respective (h k l) parameters. The average crystalline structure was determined by using Debye Scherer's Formula which is in between 14-68 nm. Fig.1 shows that the results of the diffraction pattern show the formation of cubic spinel structure for all the samples. The strongest reflection comes from (311) plane, which denotes the spinel phase, also other strongest peaks of maximum intensity was obtained from the (200) plane in all the samples due to the presence of Nacl which obtained as a byproduct (Marangoni 2012). All the compositions had spinel structures. The peaks at 31.77, 35.05, 45.47, 56.53 and 62.06 are represented as the reflection planes of (200), (311), (400), (422), (511) and (440) cubic unit cell, which corresponds to cubic spinal structure (Sanpo *et al*., 2013).

Fig.1 X ray diffraction pattern for $Co_{1-x}Mn_xFe_2O_4$ for x varying from x=0.0 to 1.0
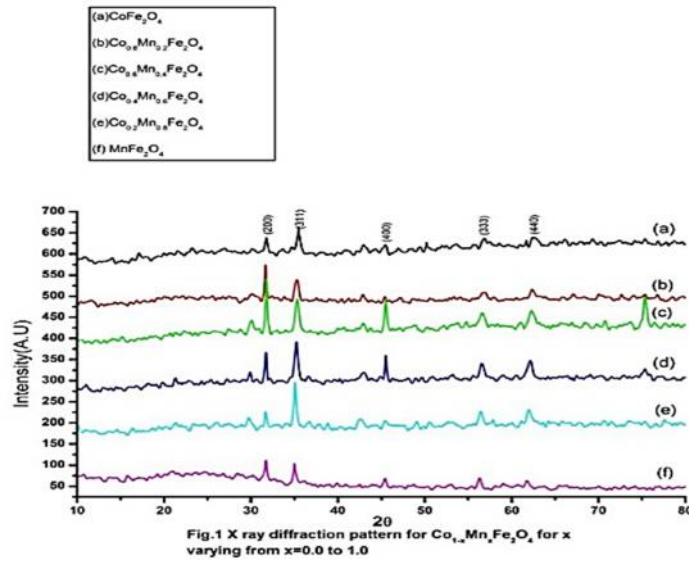
Fig 2 shows that the lattice constant calculated was found to be increased from 8.39 to 8.501 Å with the increase in manganese concentration. The lattice constant (a_o) increased with the increase in manganese content suggests the formation of compositionally homogeneous solid solution and was found to be within the range of the lattice constants of $MnFe_2O_4$ and $CoFe_2O_4$ (Vaidyanathan *et al*., 2007).
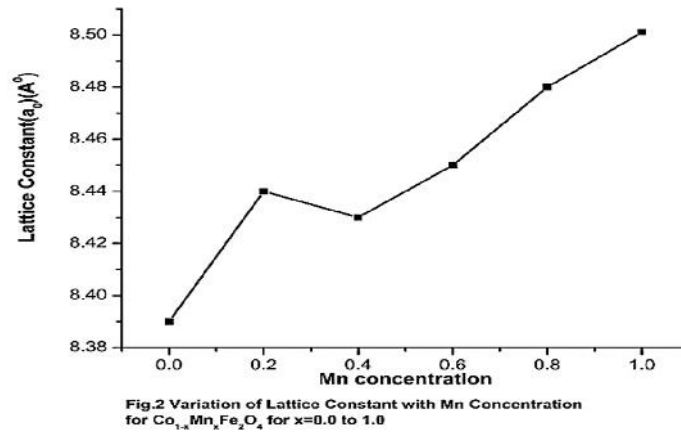

Fig.2 Variation of Lattice Constant with Mn Concentration for $Co_{1-x}Mn_xFe_2O_4$ for x=0.0 to 1.0
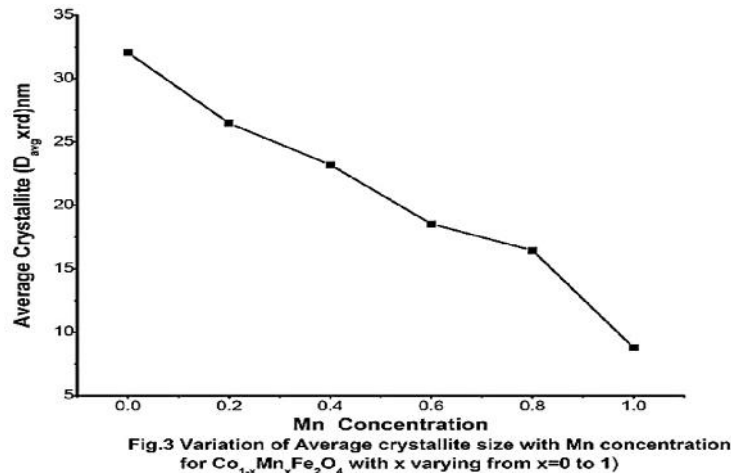
Fig 3 shows that the average crystallite size (D_{aveXRD}) decreases from 32.06 to 8.772 nm, also the crystallite size (D_{XRD}) was estimated by the Debye -Scherrer formula [14] by using the full width at half maximum value of the respective indexed peaks.

Fig.3 Variation of Average crystallite size with Mn concentration for $Co_{1-x}Mn_xFe_2O_4$ with x varying from x=0 to 1)

Vibrating Sample Magnetometer

Magnetic characterizations of the samples were measured at room temperature by vibrating sample magnetometer. The applied maximum strength of magnetization field was varied in between 20000G to 20000G and the displayed output in the form of magnetic moment which was measured around 1000emu. All the samples showed variations in specific saturation magnetization (M_s), retentivity (M_r) and coercivity (H_{ci}) as a function of Manganese substitutions. Fig 4 shows that the variation of saturation magnetization (M_s) as a function of manganese substitution and the retentivity (M_r) decreases gradually due to manganese substitution, coercivity (H_{ci}). In Ferrimagnetic spinels of cubic structure, the magnetic order is mainly due to super exchange interaction mechanism occurring between the metal ion in the A and B sub lattices The substitution of nonmagnetic ion such as manganese, which has a preferentially A site occupancy results in the reduction of the exchange interaction between A and B sites (Singhal, 2010). Hence, by varying the amount of manganese substitution, it should be possible to vary magnetic properties of the samples. The saturation magnetization (M_s) increases for the samples $Co_{0.6}Mn_{0.4}Fe_2O_4$, $Co0.4Mn0.6Fe_2O_4$, $Co_{0.2}Mn_{0.8}Fe_2O_4$ from 0.60484emu to 0.96310emu and for $MnFe_2O_4$ saturation magnetization decreases (M_s) to 0.57442emu. This is due to the addition of manganese (M^{2+}), the exchange interaction between A and B sites lowered results in strengthening of B-B interaction and weakening of A-B interaction due to which the saturation magnetization decreased. From hysteresis curve it is clear that the coercivity (H_{ci}) and retentivity (Mr) decreases to a low value shows that the particles are super paramagnetic at room temperature (Vaidyanathan *et al*., 2007).
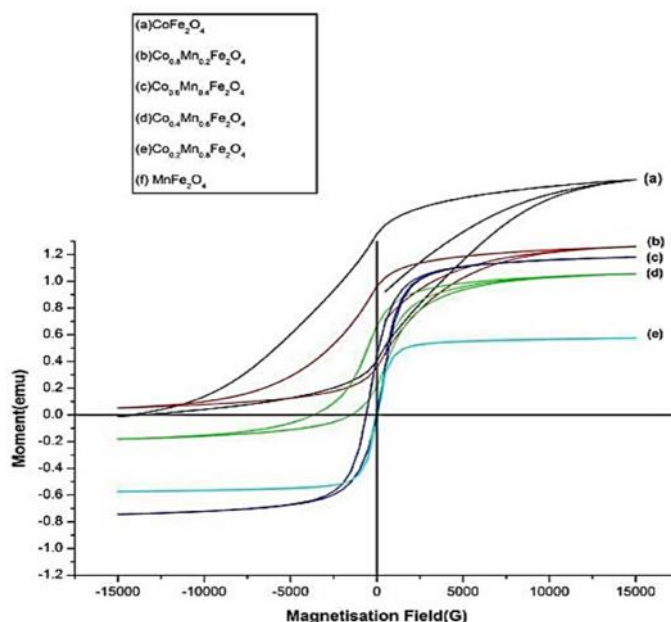

FIGURE 4. VSM variations in specific saturation magnetization of $Co_{0.6}Mn_{0.4}Fe_2O_4$, $Co0.4Mn0.6Fe2O4$ and $Co_{0.2}Mn_{0.8}Fe_2O_4$

FTIR Spectra

The FTIR spectra for $Co_{1-x}Mn_xFe_2O_4$ with x = 0.0, 0.2, 0.4, 0.6, 0.8 and 1 are shown in Fig 5. When comparing the obtained FTIR spectra of $Co_{1-x}Mn_xFe_2O_4$ for x = 0.0, 0.2, 0.4, 0.6, 0.8 and 1.0, with the previous FTIR data, (Miller and Wilkins, 1952) spectral similarities can be observed. The observed absorption vibration bands between 3779 - 3307 cm^{-1} corresponds to O-H stretching vibrations which correspond to the hydroxyl groups. Here the hydroxyl groups binds to the iron oxide surface and the water molecules chemically adsorbed to the magnetic particle surface (Pradeep, and Chandrasekaran, 2006; Wu, *et al*., 2011).The absorption bands in the range 1580-1624 cm^{-1}.corresponds to the in-plane bending vibrations of hydroxyl groups (Pradeep, and Chandrasekaran, 2006).

The absorption bands appeared in between 980 - 862 cm^{-1} shows the presence of out-of-plane bonds (Wu *et al*., 2001). From the results, it appears that the hydroxyl groups are retained in the samples during the preparation of the uncoated $Co_{1-x}Mn_xFe_2O_4$ spinel ferrites prepared by coprecipitation method. The frequency bands in the range 591-571 cm^{-1} and 435-412 cm^{-1} are attributed to the tetrahedral and octahedral structural vibrations which confirm the presence of metal oxide stretching band in ferrites (Singhal *et al*., 2010). The vibrational modes of tetrahedral structures are greater when compared to octahedral structures and it is responsible for shorter bond length of tetrahedral structures. The observed vibrations in between 591-571 cm^{-1} correspond to the metal-oxygen bonds may be due to CoO, MnO and Fe_3O_4.
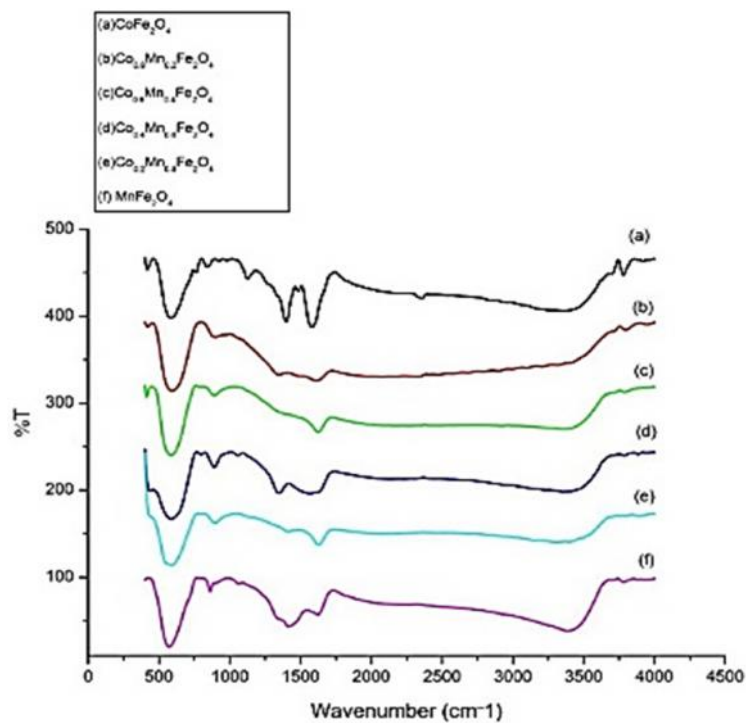
FIGURE 5. The FTIR spectra for $Co_{1-x}Mn_xFe_2O_4$ with x = 0.0, 0.2, 0.4, 0.6, 0.8 and 1

Scanning Electron Microscopy
Figure 6 shows the size of magnetic nanoparticles of $Co_{1-x}Mn_xFe_2O_4$ prepared by co-precipitation method. From the SEM photographs, it was understood that the sample consists of homogenous grain size particles of average size in between 97.31nm to 68.31nm which is in good agreement with general fixation that the particles should be within 100nm. It was found that the grains present jointly with each other. It was understood that, $Co_{1-x}Mn_xFe_2O_4$ sample synthesized through co-precipitation process resulted in low particle size.
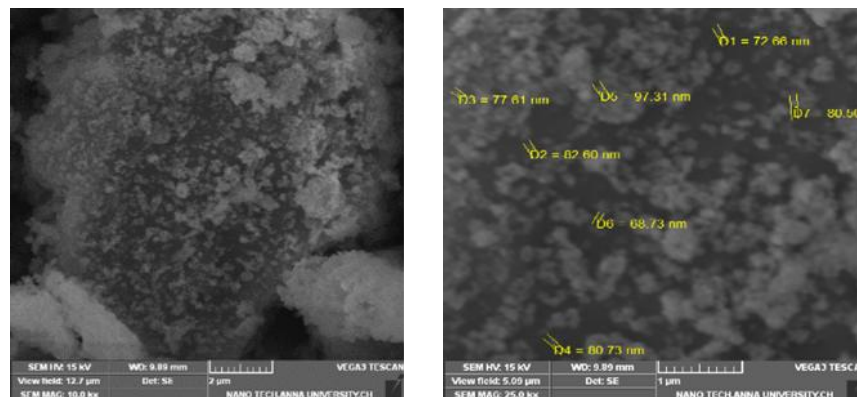

FIGURE 6. SEM Photograph Size of Iron oxide nanoparticles prepared by co-precipitation method

Growth kinetic study by iron oxide nanoparticles
Fig 7 and 8 shows that in the presence of iron oxide nanoparticles growth of both *B.subtilis* and *E. coli* strain is inhibited. *IONPs* show more antimicrobial activity to *B. subtilis* and *E. coli*. Ismail *et al*., 2015 study that *IONPs* are very prominent in biomedicine, antibacterial properties and super paramagnetic nature. Gordon *et al*., 2011 reported that the antibacterial activity of these iron oxide nanoparticles was found to be higher the antibacterial activity against *S. aureus* was significantly higher in *E. coli*.
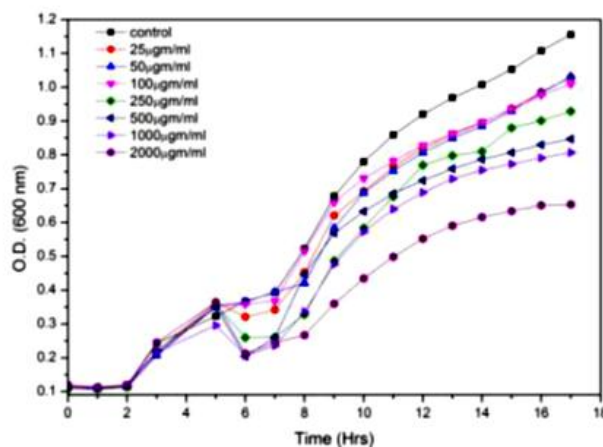
FIGURE 8. Growth kinetics of *E. coli* in the presence of iron oxide nanoparticle

Phase Contrast Microscopy
The bacterial cells clump together when it comes in contact with the *IONPs* where as there is significant change in the presence of *IONPs*. Velusamy *et al*., 2015 reported that IONPs showed a potent biofilm inhibitory effect in the case of *S. aureus* and a less significant effect in *P. aeruginosa* was achieved by using external magnetic target and confirmed in fluorescence microscopy.
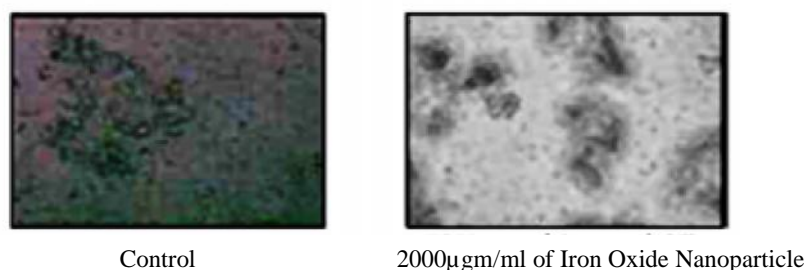

Control   2000μgm/ml of Iron Oxide Nanoparticle

FIGURE 9. Phase contrast microscopy of *E. coli*

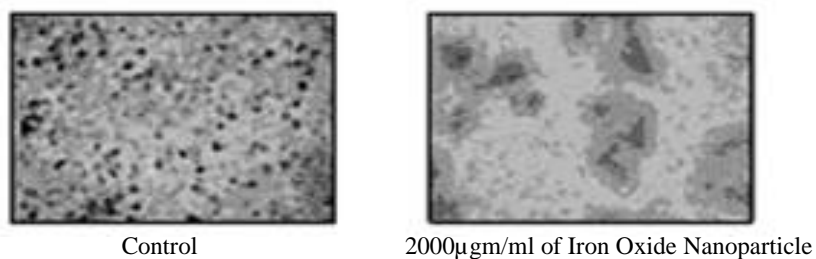Control   2000μgm/ml of Iron Oxide Nanoparticle

FIGURE 10. Phase contrast microscopy of *B. subtilis*

CONCLUSION
The present study confirmed the use of $CoCl_2$, $MnCl_2$ and $FeCl_3$ mixtures respectively in NaOH solution for the synthesis of metal substituted magnetic nanoparticles is being considered as the simplest co-precipitation method which has been confirmed and preparation of $Co_{1-x}Mn_x Fe_2O_4$ is reported by varying x=0.0 to 1.0. The rapid synthesis of *IONPs* would be suitable for developing large scale productions to process simpler and easier for downstream processing. The present research work showed that the synthesized nanostructure by this process is ready for the application in the field of nanomedicine against multidrug resistant clinical pathogens such as *E. coli and B. subtilis*. Further studies are required on understanding the cellular and molecular mechanism of iron oxide nanoparticles and the effect of microbes are of the essence to clinical applications.

REFERENCES
Dong, C. (1999) Powder X: Windows-95-based program for powder X-ray diffraction data processing. *Journal of Applied Crystallography*, 32(4), 838-838.

Gordon, T., Perlstein, B., Houbara, O., Felner, I., Banin, E., and Margel, S. (2011) Synthesis and characterization of zinc/iron oxide composite nanoparticles and their antibacterial properties. *Colloids and Surfaces A: Physicochemical and Engineering Aspects*, 374(1), 1-8.

Gupta, A.K. & Gupta, M. (2005) Synthesis and surface engineering of iron oxide nanoparticles for biomedical applications. *Biomaterials*, 26(18), 3995-4021.

Ismail, R.A., Sulaiman, G.M., Abdulrahman, S.A. & Marzoog, T.R. (2015) Antibacterial activity of magnetic iron oxide nanoparticles synthesized by laser ablation in liquid. *Materials Science and Engineering: C*, *53*, 286-297.

Jamon, D., Donatini, F., Siblini, A., Royer, F., Perzynski, R., Cabuil, V., and Neveu, S. (2009) Experimental investigation on the magneto-optic effects of ferrofluids via dynamic measurements. *Journal of Magnetism and Magnetic Materials*, *321*(9), 1148-1154.

Kim, D.H., Nikles, D.E., Johnson, D.T., and Brazel, C.S. (2008) Heat generation of aqueously dispersed $CoFe_2O_4$ nanoparticles as heating agents for magnetically activated drug delivery and hyperthermia. *Journal of Magnetism and Magnetic Materials*, *320*(19), 2390-2396.

Kluchova, K., Zboril, R., Tucek, J., Pecova, M., Zajoncova, L., Safarik, I., and Petridis, D. (2009) Superparamagnetic maghemite nanoparticles from solid-state synthesis–their functionalization towards peroral MRI contrast agent and magnetic carrier for trypsin immobilization. *Biomaterials*, 30(15), 2855-2863.

Laurent, S., Forge, D., Port, M., Roch, A., Robic, C., Vander Elst, L. & Muller, R.N. (2008) Magnetic iron oxide nanoparticles: synthesis, stabilization, vectorization, physicochemical characterizations, and biological applications. *Chemical reviews*, *108*(6), 2064-2110.

Liu, C., Zou, B., Rondinone, A. J. & Zhang, Z. J. (2000) Reverse micelle synthesis and characterization of superparamagnetic MnFe2O4 spinel ferrite nano crystallites. *The Journal of Physical Chemistry B*, *104*(6), 1141-1145.

Marangoni, A.G. (2012) *Structure-function analysis of edible fats*. Champaign: AOCS Press

Miller, F.A. & Wilkins, C.H. (1952) Infrared spectra and characteristic frequencies of inorganic ions. *Analytical Chemistry*, *24*(8), 1253-1294.

Morais, P.C., Garg, V.K., Oliveira, A.C., Silva, L.P., Azevedo, R.B., Silva, A.M.L. & Lima, E.C.D. (2001) Synthesis and characterization of size-controlled cobalt-ferrite-based ionic ferrofluids. *Journal of Magnetism and Magnetic Materials*, *225*(1), 37-40.

Paulsen, J.A., Ring, A.P., Lo, C.C.H., Snyder, J.E. & Jiles, D.C. (2005) Manganese-substituted cobalt ferrite

magnetostrictive materials for magnetic stress sensor applications. *Journal of Applied Physics*, 97(4), 044502.

Pileni, M.P. (2001) Magnetic fluids: fabrication, magnetic properties, and organization of nanocrystals. *Advanced Functional Materials*, 11(5), 323-336.

Pradeep, A. & Chandrasekaran, G. (2006) FTIR study of Ni, Cu and Zn substituted nano-particles of $MgFe_2O_4$. *Materials Letters*, *60*(3), 371-374.

Sanpo, N., Berndt, C.C., Wen, C. & Wang, J. (2013) Transition metal-substituted cobalt ferrite nanoparticles for biomedical applications. *Acta biomaterialia*, 9(3), 5830-5837.

Seil, J.T. & Webster, T.J. (2012) *Antimicrobial applications of nanotechnology: methods and literature.* International journal of nanomedicine. 7: p. 2767.

Singhal, S., Namgyal, T., Bansal, S. & Chandra, K. (2010) Effect of Zn substitution on the magnetic properties of cobalt ferrite nano particles prepared via sol-gel route. *Journal of Electromagnetic Analysis and Applications*, 2, 376-381.

Stoimenov, P.K., Klinger, R.L., Marchin, G.L. & Klabunde, K.J. (2002) Metal oxide nanoparticles as bactericidal agents. *Langmuir*, *18*(17), 6679-6686.

Sugimoto, M. (1999) The past, present, and future of ferrites. *Journal of the American Ceramic Society*, 82(2), 269-280.

Vaidyanathan, G., Sendhilnathan, S. & Arulmurugan, R. (2007) Structural and magnetic properties of Co 1– xZn x Fe_2O_4 nanoparticles by co-precipitation method. *Journal of Magnetism and Magnetic Materials*, 313(2), 293-299.

Velmurugan, V., Arunachalam, G. and Ravichandran, V. (2010) *Antibacterial activity of stem bark of Prosopis cineraria (Linn.) Druce.* Archives of Applied Science Research. 2(4): p. 147-150.

Velusamy, P., Chia-Hung, S., Shritama, A., Kumar, G.V., Jeyanthi, V. & Pandian, K. (2015) Synthesis of oleic acid coated iron oxide nanoparticles and its role in anti-biofilm activity against clinical isolates of bacterial pathogens. *Journal of the Taiwan Institute of Chemical Engineers*.

Wu, H., Liu, G., Wang, X., Zhang, J., Chen, Y., Shi, J., and Yang, S. (2011) Solvothermal synthesis of cobalt ferrite nanoparticles loaded on multiwall carbon nanotubes for magnetic resonance imaging and drug delivery. *Acta biomaterialia*, 7(9), 3496-3504.

Zhang, Y. & Zhang, J. (2005) *Surface modification of monodisperse magnetite nanoparticles for improved intracellular uptake to breast cancer cells.* Journal of colloid and interface science. 283(2): p. 352-357.

Zhen, L., He, K., Xu, C.Y. & Shao, W.Z. (2008) Synthesis and characterization of single-crystalline $MnFe_2O_4$ nanorods via a surfactant-free hydrothermal route. *Journal of Magnetism and Magnetic Materials*, 320(21), 2672-2675.